PHYSICAL REVIEW D **78,** 073009 (2008)

Limits on ν_e and $\bar{\nu}_e$ disappearance from Gallium and reactor experiments

Mario A. Acero,[1,2,3] Carlo Giunti,[2] and Marco Laveder[4]

[1]*Dipartimento di Fisica Teorica, Università di Torino, Via P. Giuria 1, I–10125 Torino, Italy*

[2]*INFN, Sezione di Torino, Via P. Giuria 1, I–10125 Torino, Italy*

[3]*Laboratoire d'Annecy-le-Vieux de Physique Thórique LAPTH, Université de Savoie, CNRS/IN2P3, 74941 Annecy-le-vieux, France*

[4]*Dipartimento di Fisica "G. Galilei," Università di Padova, and INFN, Sezione di Padova, Via F. Marzolo 8, I–35131 Padova, Italy*

(Received 16 July 2008; published 16 October 2008)

The deficit observed in the Gallium radioactive source experiments is interpreted as a possible indication of the disappearance of electron neutrinos. In the effective framework of two-neutrino mixing we obtain $\sin^2 2\vartheta \gtrsim 0.03$ and $\Delta m^2 \gtrsim 0.1$ eV^2. The compatibility of this result with the data of the Bugey and Chooz reactor short-baseline antineutrino disappearance experiments is studied. It is found that the Bugey data present a hint of neutrino oscillations with $0.02 \lesssim \sin^2 2\vartheta \lesssim 0.08$ and $\Delta m^2 \approx 1.8$ eV^2, which is compatible with the Gallium allowed region of the mixing parameters. This hint persists in the combined analyses of Bugey and Chooz data, of Gallium and Bugey data, and of Gallium, Bugey, and Chooz data.

DOI: 10.1103/PhysRevD.78.073009 PACS numbers: 14.60.Pq, 14.60.Lm, 14.60.St

I. INTRODUCTION

The observation of solar and very-long-baseline reactor neutrino oscillations due to the squared-mass difference $\Delta m^2_{\mathrm{SOL}} = (7.59 \pm 0.21) \times 10^{-5}$ eV^2 [1] and the observation of atmospheric and long-baseline accelerator neutrino oscillations due to the squared-mass difference $\Delta m^2_{\mathrm{ATM}} = 2.74^{+0.44}_{-0.26} \times 10^{-3}$ eV^2 [2] give very robust evidence of three-neutrino mixing (for reviews of the theory and phenomenology of neutrino mixing, see Refs. [3–11]). There are, however, some anomalies in the data of neutrino experiments which could be interpreted as indications of exotic neutrino physics beyond three-neutrino mixing: the LSND anomaly [12], the Gallium radioactive source experiments anomaly [13], and the MiniBooNE low-energy anomaly [14]. In this paper we consider the anomaly observed in the Gallium radioactive source experiments [13,15–18], in which the Gallium solar neutrino detectors GALLEX [19] and SAGE [20] were tested by measuring the electron neutrino flux produced by intense artificial radioactive sources placed inside the detectors. The Gallium radioactive source experiments measured a number of events smaller than expected. This deficit can be interpreted[1] as an indication of the disappearance of electron neutrinos due to neutrino oscillations [22–24]. Under this hypothesis, we analyze the data of the Gallium radioactive source experiments in the effective framework of two-neutrino mixing, which describes neutrino oscillations due to a Δm^2 that is much larger than the solar and atmospheric ones (see Refs. [5,6,11]). We also study the compatibility of this interpretation of the Gallium radioactive source experiments anomaly with the data of the Bugey [25] and Chooz [26] reactor short-baseline antineutrino disappearance experiments.

II. GALLIUM

The GALLEX [19] and SAGE [20] solar neutrino detectors (see Refs. [3–11]) have been tested in so-called "Gallium radioactive source experiments" which consist in the detection of electron neutrinos produced by intense artificial ^{51}Cr and ^{37}Ar radioactive sources placed inside the detectors.

The radioactive nuclei ^{51}Cr and ^{37}Ar decay through electron capture ($e^- + {}^{51}\mathrm{Cr} \to {}^{51}\mathrm{V} + \nu_e$ and $e^- + {}^{37}\mathrm{Ar} \to {}^{37}\mathrm{Cl} + \nu_e$) emitting ν_e lines with the energies and branching ratios listed in Table I. These neutrinos were detected through the same reaction used for the detection of solar neutrinos [28]:

$$\nu_e + {}^{71}\mathrm{Ga} \to {}^{71}\mathrm{Ge} + e^-, \tag{1}$$

which has the low neutrino energy threshold $E_\nu^{\mathrm{th}}({}^{71}\mathrm{Ga}) = 0.233$ MeV. The cross sections of the ν_e lines emitted in ^{51}Cr and ^{37}Ar decay interpolated from Table II of Ref. [27] are listed in Table I.

The ratios R of measured and predicted ^{71}Ge production rates in the two GALLEX ^{51}Cr radioactive source experiments,[2] Cr1 [15] and Cr2 [16], and the SAGE ^{51}Cr [17,18] and ^{37}Ar [13] radioactive source experiments, as reported

[1]Another possible explanation is that the theoretical cross section of the Gallium detection process has been overestimated [13,21].

[2]As explained in Ref. [13], the values of R in Table II for the two GALLEX ^{51}Cr radioactive source experiments are different from those published in Refs. [15,16], because of an improved reanalysis of the data. Similar results have been published recently in a PhD thesis [29] and discussed at the Neutrino 2008 Conference [30]: $R(\mathrm{Cr1}) = 0.997 \pm 0.11$ and $R(\mathrm{Cr2}) = 0.807^{+0.11}_{-0.10}$ in a standard rise-time analysis; $R(\mathrm{Cr1}) = 0.953 \pm 0.11$ and $R(\mathrm{Cr2}) = 0.812^{+0.10}_{-0.11}$ in a pulse-shape analysis. We have verified that our results are stable against such small changes of the data.

TABLE I. Energies (E_ν), branching ratios (B.R.) and Gallium cross sections (σ) of the ν_e lines emitted in ^{51}Cr and ^{37}Ar decay through electron capture. The cross sections are interpolated from Table II of Ref. [27].

	^{51}Cr				^{37}Ar	
E_ν [keV]	747	752	427	432	811	813
B.R.	0.8163	0.0849	0.0895	0.0093	0.902	0.098
$\sigma[10^{-46}$ cm$^2]$	60.8	61.5	26.7	27.1	70.1	70.3

in Ref. [13], are listed in Table II. Since the weighted average, [13]

$$R_{\rm Ga} = 0.88 \pm 0.05, \tag{2}$$

is smaller than unity by more than 2σ, it can be interpreted as an indication of the disappearance of electron neutrinos due to neutrino oscillations [22–24]. The χ^2 in the absence of oscillation is 8.19 for 4 degrees of freedom, corresponding to a 8.5% goodness-of-fit,[3] as shown in Table III. Therefore, a fluctuation of the data in the case of no oscillations cannot be excluded. However, since from a physical point of view it is interesting to explore possible indications of nonstandard physics, in the following we consider the case of neutrino oscillations.

In the effective framework of two-neutrino oscillations, which is appropriate in the case of short-baseline oscillations generated by a squared-mass difference much larger than $\Delta m^2_{\rm SOL}$ and $\Delta m^2_{\rm ATM}$ (see Refs. [5,11]), the survival probability of electron neutrinos and antineutrinos with energy E_ν at a distance L from the source is given by[4]

$$P_{\overset{(-)}{\nu}_e \to \overset{(-)}{\nu}_e}(L, E_\nu) = 1 - \sin^2 2\vartheta \sin^2\left(\frac{\Delta m^2 L}{4E_\nu}\right), \tag{3}$$

where ϑ is the mixing angle and Δm^2 is the squared-mass difference. The fit of the data gives information on the values of the mixing parameters $\sin^2 2\vartheta$ and Δm^2.

In our calculation, the theoretical value of the ratio R of the predicted ^{71}Ge production rates in each of the Gallium radioactive source experiments in the cases of presence and absence of neutrino oscillations is given by

[3]The goodness-of-fit is the probability to obtain a worse fit under the assumption that the model under consideration is correct (see Ref. [31]). It is the standard statistic used for the estimation of the quality of a fit obtained with the least-squares method, assuming the validity of the approximation in which $\chi^2_{\rm min}$ has a χ^2 distribution with NDF $= N_{\rm D} - N_{\rm P}$ degrees of freedom, where $N_{\rm D}$ is the number of data points and $N_{\rm P}$ is the number of fitted parameters. The fit is usually considered to be acceptable if the goodness-of-fit is larger than about 1%.

[4]The symmetry under CPT transformations, which is a characteristic of all relativistic local quantum field theories, implies that the survival probabilities of neutrinos and antineutrinos are equal (see Ref. [11]).

TABLE II. Ratios R of measured and predicted ^{71}Ge production rates in the two GALLEX ^{51}Cr radioactive source experiments, Cr1 [15] and Cr2 [16], and the SAGE ^{51}Cr [17,18] and ^{37}Ar [13] radioactive source experiments, as reported in Ref. [13]. We give also the radii and heights of the GALLEX and SAGE cylindrical detectors and the heights from the base of the detectors at which the radioactive sources were placed along the axes of the detectors.

	GALLEX		SAGE	
	Cr1	Cr2	^{51}Cr	^{37}Ar
R	1.00 ± 0.10	0.81 ± 0.10	0.95 ± 0.12	0.79 ± 0.10
radius [m]	1.9		0.7	
height [m]	5.0		1.47	
source height [m]	2.7	2.38	0.72	

$$R = \frac{\int dV L^{-2} \sum_i ({\rm B.R.})_i \sigma_i P_{\nu_e \to \nu_e}(L, E_{\nu,i})}{\sum_i ({\rm B.R.})_i \sigma_i \int dV L^{-2}}, \tag{4}$$

where i is the index of the ν_e lines emitted in ^{51}Cr or ^{37}Ar, which are listed in Table I. The measured ratios are listed in Table II, together with the dimensions of the detectors, which we approximate as cylindrical, and the height from the base of each detector at which the radioactive sources were placed along the axis of the respective detector. We averaged the neutrino path length L with a Monte Carlo integration over the volume V of each cylindrical detector.

In the separate analysis of the result of each Gallium radioactive source experiment in terms of neutrino oscillations, the two mixing parameters cannot be determined through a least-squares analysis from one data point. Therefore, we adopt a Bayesian approach, as done in Ref. [33], considering R as a random variable with a uniform prior probability distribution between zero and one. Then, if $R_{\rm obs}$ is the observed value of R, the normalized posterior probability distribution of R is given by

$$p(R|R_{\rm obs}) = \frac{p(R_{\rm obs}|R)}{\int_0^1 dR\, p(R_{\rm obs}|R)}. \tag{5}$$

Here, $p(R_{\rm obs}|R)$ is the sampling distribution of $R_{\rm obs}$ given R, which we assume to be Gaussian with standard deviation equal to the experimental uncertainty. The allowed interval of R with a given Bayesian confidence level is given by the highest posterior density interval with integrated probability equal to the confidence level. Figure 1 shows the resulting allowed regions in the $\sin^2 2\vartheta - \Delta m^2$ plane. One can see that the first GALLEX source experiment (Cr1) and the ^{51}Cr SAGE source experiment, in which the measured rate is within 1σ from unity, imply only upper limits for the mixing parameters. On the other hand, the analyses of the second GALLEX source experiment (Cr2) and the ^{37}Ar SAGE source experiment give 2σ allowed bands, which have a large overlap for $\Delta m^2 \gtrsim 1$ eV^2.

TABLE III. Values of $\chi^2_{\rm min}$, number of degrees of freedom (NDF) and goodness-of-fit (GoF) for the fit of different combinations of the results of the Gallium radioactive source experiments and the Bugey and Chooz reactor experiments. The first three lines correspond to the case of no oscillations (No Osc.). The following five lines, including the best-fit values of $\sin^2 2\vartheta$ and Δm^2, correspond to the case of oscillations (Osc.). The last three lines describe the parameter goodness-of-fit (PG) [32].

		Ga	Bu	Ga + Bu	Bu + Ch	Ga + Ch	Ga + Bu + Ch
No Osc.	$\chi^2_{\rm min}$	8.19	50.94	59.13	51.00	8.26	59.19
	NDF	4	55	59	56	5	60
	GoF	0.085	0.63	0.47	0.66	0.14	0.51
Osc.	$\chi^2_{\rm min}$	2.94	47.97	53.87	48.63	6.60	54.80
	NDF	2	53	57	54	3	58
	GoF	0.23	0.67	0.59	0.68	0.086	0.60
	$\sin^2 2\vartheta_{\rm bf}$	0.22	0.048	0.062	0.041	0.08	0.60
	$\Delta m^2_{\rm bf}$ [eV^2]	1.98	1.85	1.85	1.85	1.72	1.85
PG	$\Delta\chi^2_{\rm min}$			2.98	0.59	3.63	3.85
	NDF			2	1	1	3
	GoF			0.23	0.44	0.057	0.28

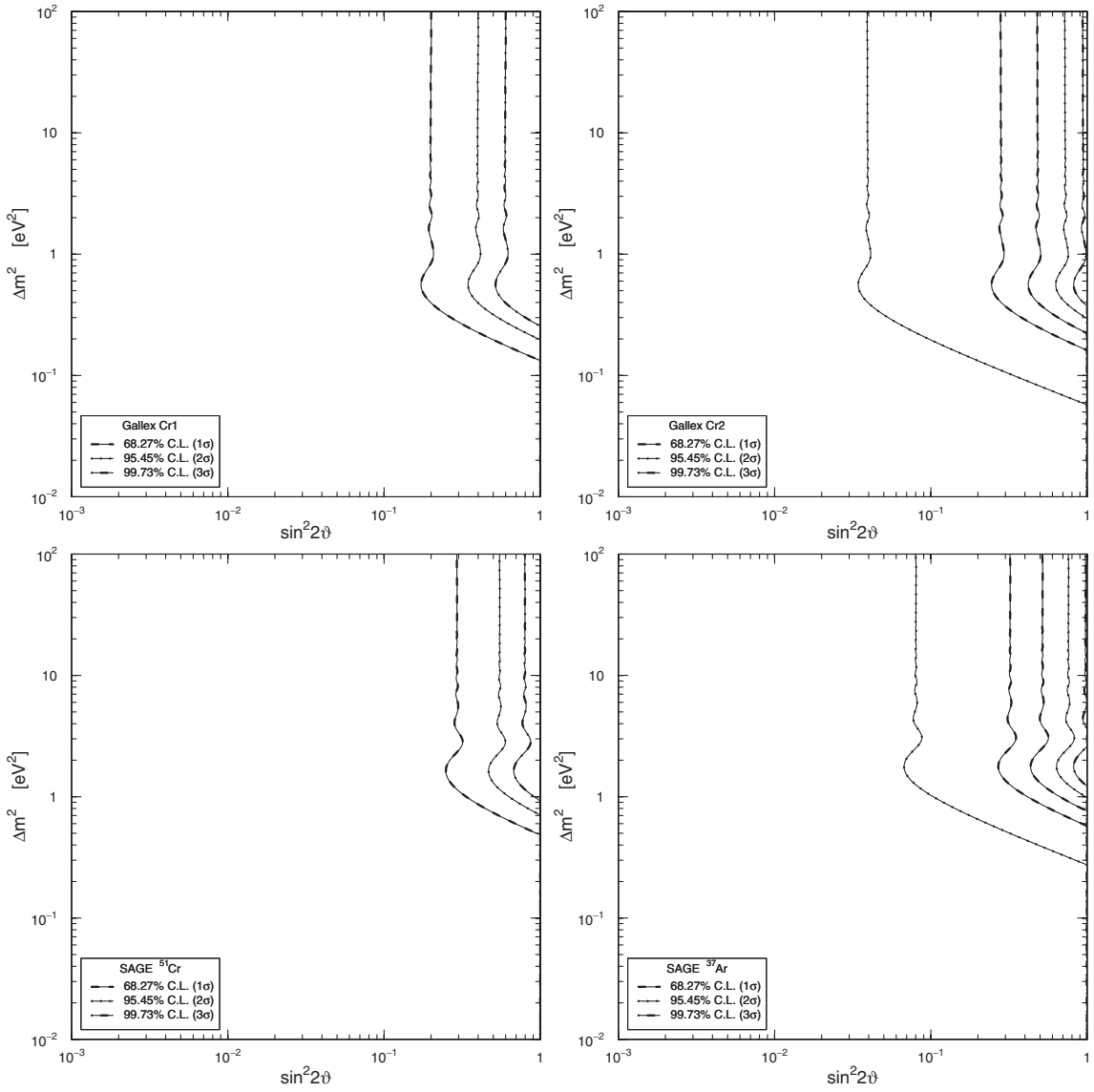

FIG. 1. Allowed regions in the $\sin^2 2\vartheta - \Delta m^2$ plane obtained from the fits of the results of the two GALLEX ^{51}Cr radioactive source experiments, Cr1 and Cr2, and the SAGE ^{51}Cr and ^{37}Ar radioactive source experiments. The curves in the GALLEX Cr1 and SAGE ^{51}Cr plots exclude the region on the right. In the GALLEX Cr2 and SAGE ^{37}Ar plots, the pairs of 1σ and 2σ curves delimit allowed regions, whereas the 3σ curves exclude the region on the right.

Let us now discuss the combined fit of the four Gallium source experiments. Since there are enough data points to determine the two mixing parameters $\sin^2 2\vartheta$ and Δm^2, we abandon the Bayesian approach in favor of a standard frequentist least-squares fit. This method is based on a global minimization of the χ^2 in the $\sin^2 2\vartheta - \Delta m^2$ plane and the calculation of the Confidence Level contours corresponding to a $\Delta\chi^2$ with 2 degrees of freedom: $\Delta\chi^2 = 2.30$, 6.18, 11.83 for 68.27% (1σ), 95.45% (2σ) and 99.73% (3σ) C.L., respectively, (see Ref. [31]).

The result of the combined least-squares analysis of the four Gallium source experiments is shown in Fig. 2. One can see that there is an allowed region in the $\sin^2 2\vartheta - \Delta m^2$ plane at 1σ for $\Delta m^2 \gtrsim 0.6\ \mathrm{eV}^2$ and $0.08 \lesssim \sin^2 2\vartheta \lesssim 0.4$. The values of χ^2_{min}, the number of degrees of freedom (NDF), the goodness-of-fit (GoF) and the best-fit values of the mixing parameters are given in Table III. The value of the goodness-of-fit (23%) shows that the fit is acceptable.

Table IV shows the allowed ranges of $\sin^2 2\vartheta$ and Δm^2 obtained from the corresponding marginal $\Delta\chi^2 \equiv \chi^2 - \chi^2_{\mathrm{min}}$ in Fig. 2. The presence of 2σ lower limits for $\sin^2 2\vartheta$ and Δm^2 in spite of the absence of a 2σ lower limit in the $\sin^2 2\vartheta - \Delta m^2$ plane in Fig. 2 is an effect due to the statistical analysis: for one parameter 2σ corresponds to $\Delta\chi^2 = 4$, whereas for two parameters it corresponds to $\Delta\chi^2 = 6.18$. Hence, it is fair to conclude that there is an indication of a possible neutrino disappearance due to neutrino oscillations with $\sin^2 2\vartheta \gtrsim 0.03$ and $\Delta m^2 \gtrsim 0.1\ \mathrm{eV}^2$ at a confidence level between one and two sigmas ($\sim$ 70–90% C.L.).

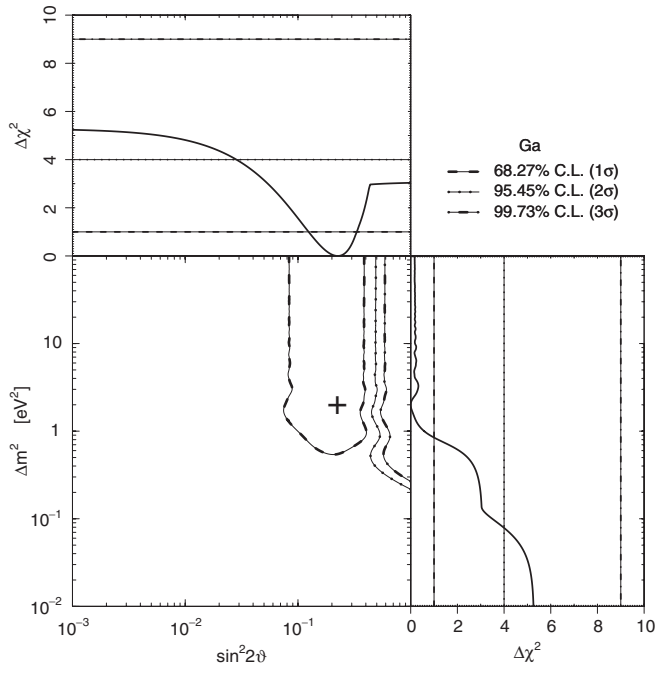

FIG. 2. Allowed regions in the $\sin^2 2\vartheta - \Delta m^2$ plane and marginal $\Delta\chi^2$'s for $\sin^2 2\vartheta$ and Δm^2 obtained from the combined fit of the results of the two GALLEX ^{51}Cr radioactive source experiments and the SAGE ^{51}Cr and ^{37}Ar radioactive source experiments. The best-fit point corresponding to χ^2_{min} is indicated by a cross.

TABLE IV. Allowed ranges of $\sin^2 2\vartheta$ and Δm^2 from the combined fit of the results of Gallium radioactive source experiments, from the fit of the results of the Bugey reactor experiment, and from the combined fit. The dots indicate the absence of limits.

Parameter	C.L.	Ga	Bu	Ga + Bu
$\sin^2 2\vartheta$	68.27%(1σ)	0.12–0.33	0.021–0.075	0.035–0.087
	95.45%(2σ)	>0.028	···	0.007–0.19
	99.73%(3σ)	···	···	···
Δm^2 [eV^2]	68.27%(1σ)	>0.85	1.77–1.91	1.79–1.91
	95.45%(2σ)	>0.079	···	>0.77
	99.73%(3σ)	···	···	···

III. BUGEY

The disappearance of electron antineutrinos have been investigated by several reactor neutrino experiments at different baselines (see Refs. [11,34]). Since, according to Eq. (3), the survival probabilities of neutrinos and antineutrinos are equal, the interpretation of the results of Gallium radioactive source experiments in terms of electron neutrino disappearance can be compared directly with the results of reactor neutrino experiments.

In this section we consider the results of the reactor short-baseline Bugey experiment [25], which put the most stringent constraints on the disappearance of electron antineutrinos due to $\Delta m^2 \gtrsim 0.1\ \mathrm{eV}^2$.

Reactor neutrino experiments detect electron antineutrinos through the inverse neutron decay process

$$\bar{\nu}_e + p \rightarrow n + e^+. \tag{6}$$

The neutrino energy E_ν and the positron kinetic energy T_e are related by

$$E_\nu = T_e + T_n + m_e + m_n - m_p \simeq T_e + 1.8\ \mathrm{MeV}, \tag{7}$$

where T_n is the negligibly small recoil kinetic energy of the neutron. In the Bugey experiment the survival probability of electron antineutrinos was measured at three source-detector distances: $L_j = 15$, 40, 95 m, for $j = 1$, 2, 3, respectively. We use the ratio of observed and expected (in the case of no oscillation) positron spectra given in Fig. 17 of Ref. [25], in which there are $N_j = 25$, 25, 10 energy bins. We analyze the data with the following χ^2, taken from Ref. [25]:

$$\chi^2 = \sum_{j=1}^{3}\left\{\sum_{i=1}^{N_j}\frac{[(Aa_j + b(E_{ji} - E_0))R_{ji}^{\rm the} - R_{ji}^{\rm exp}]^2}{\sigma_{ji}^2} + \frac{(a_j - 1)^2}{\sigma_{a_j}^2}\right\} + \frac{(A-1)^2}{\sigma_A^2} + \frac{b^2}{\sigma_b^2}, \quad (8)$$

where E_{ji} is the central energy of the ith bin in the positron kinetic energy spectrum measured at the L_j source-detector distance, $R_{ji}^{\rm exp}$ and $R_{ji}^{\rm the}$ are, respectively, the corresponding measured and calculated ratios. The uncertainties σ_{ji} include the statistical uncertainty of each bin and a 1% systematic uncertainty added in quadrature, which takes into account the uncertainty of the spectrum calculation (with a total of about 5% uncorrelated systematic uncertainty over 25 bins). The coefficients $(Aa_j + b(E_{ji} - E_0))$, with $E_0 = 1$ MeV, were introduced in Ref. [25] in order to take into account the systematic uncertainty of the positron energy calibration. The value of χ^2 as a function of $\sin^2 2\vartheta$ and Δm^2 is calculated by minimizing Eq. (8) with respect to the five parameters A, a_j $(j = 1, 2, 3)$, b, which have, respectively, uncertainties $\sigma_A = 0.048$, $\sigma_{a_j} = 0.014$ $\sigma_b = 0.02$ MeV^{-1} [25]. Following Ref. [35], we approximate the neutrino flux, the detection cross section and the detection efficiency as constants in each energy bin. Then, $R_{ji}^{\rm the}$ is given by

$$R_{ji}^{\rm the} = \frac{\int dL L^{-2}\int_{E_{ji}-\Delta E_j/2}^{E_{ji}+\Delta E_j/2} dE \int_{-\infty}^{+\infty} dT_e F(E, T_e) P_{\bar{\nu}_e \to \bar{\nu}_e}(L, E_\nu)}{\Delta E_j \int dL L^{-2}}. \quad (9)$$

Here T_e and E_ν are, respectively, the positron kinetic energy and the neutrino energy, related by Eq. (7), whereas E is the measured positron kinetic energy, which is connected to T_e by the energy resolution function of the detector $F(E, T_e)$. We considered a Gaussian energy resolution function with standard deviation $0.252\sqrt{E/4.2\ \text{MeV}}$ MeV [25]. The quantities ΔE_j are the widths of the energy bins in each detector. The integration over the neutrino path length L is performed by a Monte Carlo which takes into account the geometries of the reactor and of the detectors and their relative positions [36].

With this method we obtained the 90% C.L. raster-scan[5] exclusion curve shown in Fig. 3, which is similar to the original 90% C.L. raster-scan Bugey exclusion curve in Ref. [25].

Let us emphasize that the raster-scan method is statistically weak, because it does not have proper coverage [37]. We presented in Fig. 3 the raster-scan exclusion curve only to show by comparison with the analogous figure in Ref. [25] that our analysis of the Bugey data is acceptable. The dashed line in Fig. 3 shows the 90% C.L. Bugey exclusion curve obtained with the standard least-squares method, which we adopted also in the previous Fig. 2 and the following Figs. 4–9. From Fig. 3 one can see that the 90% C.L. raster-scan exclusion curve overcovers for all values of Δm^2, except for small intervals around $\Delta m^2 \simeq 0.9$ eV^2 and $\Delta m^2 \simeq 1.9$ eV^2.

Figure 4 shows the allowed regions in the $\sin^2 2\vartheta - \Delta m^2$ plane and the marginal $\Delta\chi^2$'s for $\sin^2 2\vartheta$ and Δm^2 obtained from the least-squares analysis of Bugey data. The value and location in the $\sin^2 2\vartheta - \Delta m^2$ plane of the minimum of the χ^2, the number of degrees of freedom (NDF) and the goodness-of-fit (GoF) are given in Table III. The fit is satisfactory, since the goodness-of-fit is 67%. The best-fit value of the oscillation parameters and the small 1σ allowed regions in Fig. 4 are in favor of neutrino oscillations. However, the 2σ and 3σ contours in Fig. 4 provide only upper limits to neutrino oscillations. Also, the value of the χ^2 in the case of absence of oscillations and the corresponding goodness-of-fit (63%) do not allow us to exclude the absence of oscillations.

The reason of the hint in favor of neutrino oscillations given by the Bugey data is illustrated in Fig. 5, where the histogram relative to the best fit is shown against the Bugey

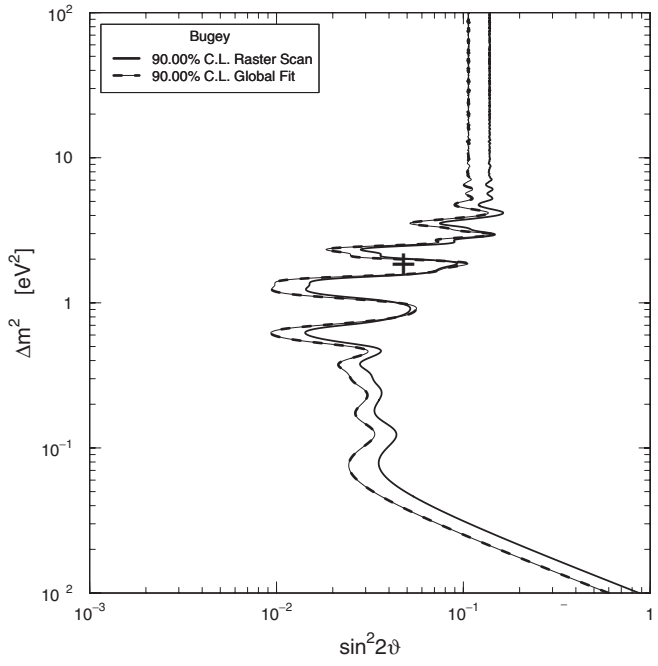

FIG. 3. 90% C.L. exclusion curves in the $\sin^2 2\vartheta - \Delta m^2$ plane obtained from a raster-scan analysis of Bugey data (solid line) and from a standard global least-squares fit (dashed line).

[5]In the raster-scan method, $\chi^2_{\rm min}$ is found for each fixed value of Δm^2. The corresponding upper limit for $\sin^2 2\vartheta$ is calculated as the value of $\sin^2 2\vartheta$ for which the cumulative distribution function of $\Delta\chi^2 \equiv \chi^2 - \chi^2_{\rm min}$, which has 1° of freedom, is equal to the confidence level ($\Delta\chi^2 = 2.71$ for 90% C.L.).

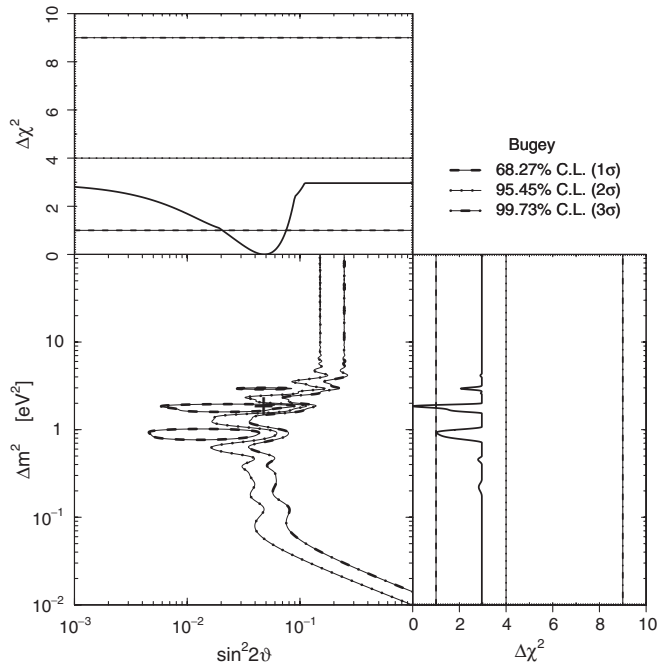

FIG. 4. Allowed regions in the $\sin^2 2\vartheta - \Delta m^2$ plane and marginal $\Delta\chi^2$'s for $\sin^2 2\vartheta$ and Δm^2 obtained from the least-squares analysis of Bugey data. The best-fit point corresponding to $\chi^2_{\rm min}$ is indicated by a cross.

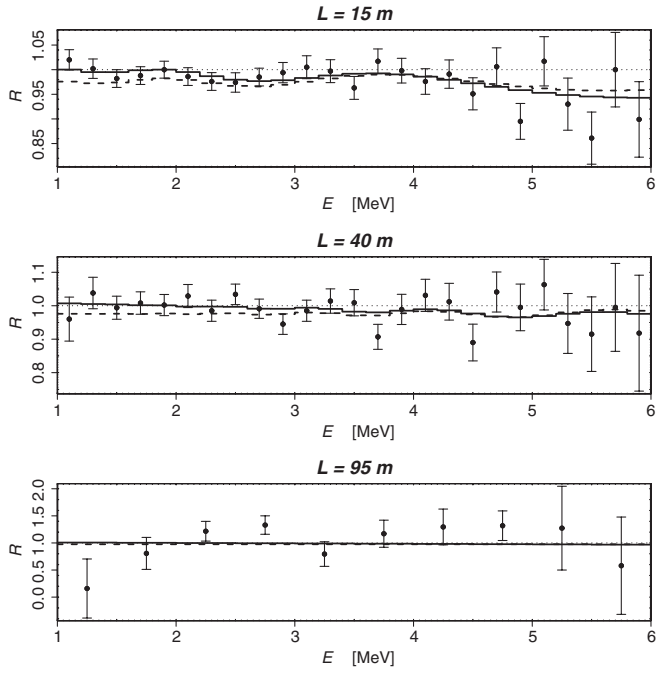

FIG. 5. Best fit of Bugey data (points with error bars [25]). The three panels show the ratio R of observed and expected (in the case of no oscillation) event rates at the three source-detector distances in the Bugey experiment as functions of the measured positron kinetic energy E [see Eq. (9)]. In each panel, the solid and dashed histograms correspond, respectively, to the best-fit values of $(Aa_j + b(E_{ji} - E_0))R^{\rm the}_{ji}$ and $R^{\rm the}_{ji}$ [see Eq. (8)].

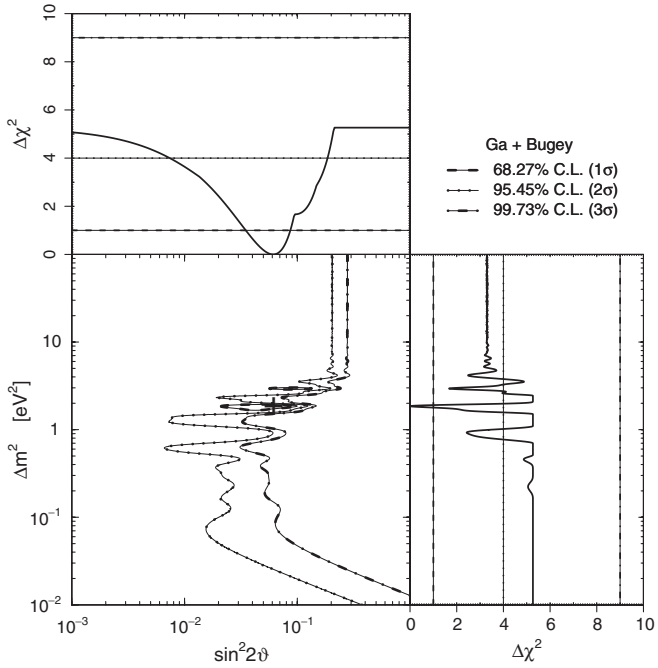

FIG. 6. Allowed regions in the $\sin^2 2\vartheta - \Delta m^2$ plane and marginal $\Delta\chi^2$'s for $\sin^2 2\vartheta$ and Δm^2 obtained from the combined fit of the results of the two GALLEX ^{51}Cr radioactive source experiments, the SAGE ^{51}Cr and ^{37}Ar radioactive source experiments and the Bugey reactor experiment. The best-fit point corresponding to $\chi^2_{\rm min}$ is indicated by a cross.

$R^{\rm exp}_{ji}$'s. With the help of the histogram, one can see that there is a weak hint of oscillations. The 1σ allowed regions in Fig. 4 have very narrow Δm^2 ranges around 0.9 eV^2, 1.85 eV^2, and 3 eV^2, because slight shifts of Δm^2 from these optimal values spoil the agreement with the data of the histogram in Fig. 5.

Table IV shows the marginal allowed ranges of $\sin^2 2\vartheta$ and Δm^2 obtained from the corresponding $\Delta\chi^2$'s in Fig. 4. One can see that there is a hint of neutrino oscillations with $0.02 \lesssim \sin^2 2\vartheta \lesssim 0.08$ and $\Delta m^2 \approx 1.8$ eV^2.

From a comparison of Figs. 2 and 4 one can see that the allowed regions of the Gallium radioactive source experiments and the Bugey experiment are marginally compatible for $\sin^2 2\vartheta \sim 0.1$ and $\Delta m^2 \gtrsim 1$ eV^2. Figure 6 shows the allowed regions obtained from the combined fit. Since the Bugey data are statistically dominant, the curves in Fig. 6 are not very different from those in Fig. 4, which have been obtained from the fit of the Bugey data alone. The inclusion of the Gallium data has the effect of eliminating the 1σ allowed region at $\Delta m^2 \approx 0.9$ eV^2 and of disfavoring at 1σ values of $\sin^2 2\vartheta$ smaller than about 2×10^{-2}. The value and location of $\chi^2_{\rm min}$, the number of degrees of freedom and the goodness-of-fit are listed in Table III. One can see that the Gallium data do not spoil the good fit of the Bugey data. Indeed, the value of the parameter goodness-

of-fit[6] [32] reported in Table III shows that the Bugey and Gallium data are compatible under the hypothesis of neutrino oscillations. The marginal allowed ranges of $\sin^2 2\vartheta$ and Δm^2 obtained from the corresponding $\Delta\chi^2$'s in Fig. 6 are given in Table IV.

IV. CHOOZ

In this section we consider the result of the long-baseline reactor neutrino experiment Chooz [26], which gives limits on neutrino oscillations which are comparable with those of the Bugey experiment for $\Delta m^2 \gtrsim 2$ eV^2.

In the Chooz experiment the ratio of the number of observed events and that expected in the absence of neutrino oscillations is

$$R_{\text{Chooz}} = 1.01 \pm 0.04. \tag{10}$$

The value of this ratio puts a constraint on the disappearance of electron (anti)neutrinos with energies in the MeV range at distances smaller than about 1 km. This corresponds to a constraint on $\sin^2 2\vartheta$ for $\Delta m^2 \gtrsim 10^{-3}$ eV^2. In the range of sensitivity of the Gallium radioactive source experiments, $\Delta m^2 \gtrsim 10^{-1}$ eV^2 (see Figs. 2), the oscillation length of reactor antineutrinos is much shorter than the Chooz source-detector distance. In this case, the Chooz experiment is only sensitive to the averaged survival probability

$$\langle P_{\overset{(-)}{\nu}_e \to \overset{(-)}{\nu}_e} \rangle = 1 - \tfrac{1}{2}\sin^2 2\vartheta. \tag{11}$$

Therefore, the Chooz result in Eq. (10) can be combined[7] with the results of the Gallium radioactive source experiments simply by considering it as a measurement of $\sin^2 2\vartheta$: in the Bayesian approach of Eq. (5)

$$\sin^2 2\vartheta < 0.071, 0.15, 0.23, \tag{12}$$

at 68.27% (1σ), 95.45% (2σ), 99.73% (3σ) Bayesian Confidence Level, respectively.

First, we performed a combined frequentist least-squares analysis of the Bugey and Chooz data, which yielded the allowed regions in the $\sin^2 2\vartheta - \Delta m^2$ plane shown in Fig. 7, the best-fit values of the mixing parameters reported in Table III, and the marginal allowed ranges listed in Table V. One can see that the addition of the Chooz result to the Bugey data analysis has the effect of improving slightly the upper limit on $\sin^2 2\vartheta$ for $\Delta m^2 \gtrsim 3$ eV^2

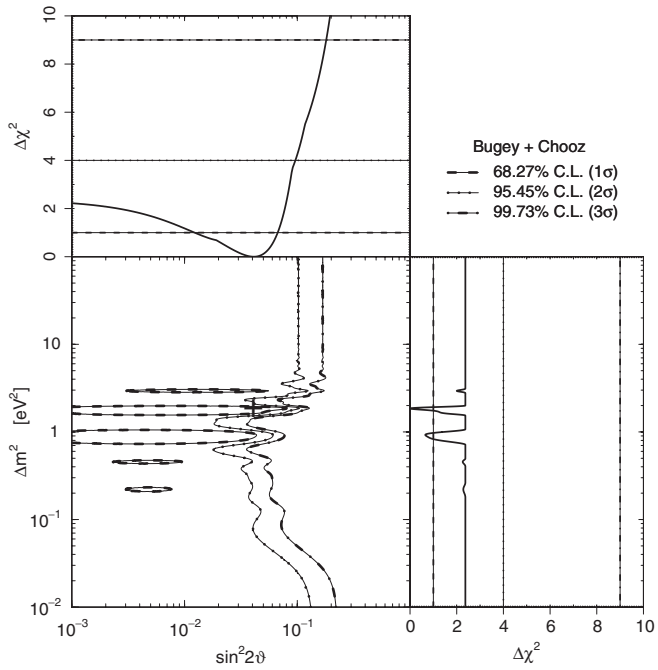

FIG. 7. Allowed regions in the $\sin^2 2\vartheta - \Delta m^2$ plane and marginal $\Delta\chi^2$'s for $\sin^2 2\vartheta$ and Δm^2 obtained from the combined fit of the results of the Bugey and Chooz reactor experiments. The best-fit point corresponding to χ^2_{min} is indicated by a cross.

and that of excluding values of $\sin^2 2\vartheta$ larger than about 0.1 for $\Delta m^2 \lesssim 3 \times 10^{-2}$ eV^2, where Bugey is not sensitive. In the intermediate range of Δm^2, where Bugey is sensitive to the oscillations, the addition of the Chooz result weakens the hint in favor of oscillations given by the Bugey data: the 1σ allowed regions in Fig. 4 are stretched towards small values of $\sin^2 2\vartheta$ in Fig. 7. However, the best-fit value of the mixing parameters remain unchanged, because of the dominance of the Bugey data. From Table III, one can see that the parameter goodness-of-fit implies that Bugey and Chooz results are compatible under the hypothesis of neutrino oscillations, but the goodness-of-fit obtained in

TABLE V. Allowed ranges of $\sin^2 2\vartheta$ and Δm^2 from the combined fit of the results of the Bugey and Chooz reactor experiments, the Gallium radioactive source and Chooz reactor experiments, and the Gallium radioactive source and the Bugey and Chooz reactor experiments. The dots indicate the absence of limits.

Parameter	C.L.	Bu + Ch	Ga + Ch	Ga + Bu + Ch
$\sin^2 2\vartheta$	68.27%(1σ)	0.012–0.067	0.017–0.14	0.028–0.078
	95.45%(2σ)	<0.096	<0.20	0.002–0.12
	99.73%(3σ)	<0.18	<0.26	<0.18
Δm^2 [eV^2]	68.27%(1σ)	0.83–1.92	>0.62	1.78–1.91
	95.45%(2σ)	...	...	>0.74
	99.73%(3σ)	...	...	...

[6]The value of $(\Delta\chi^2_{\text{min}})_{\text{A+B}}$ corresponding to the parameter goodness-of-fit of two experiments A and B is given by $(\chi^2_{\text{min}})_{\text{A+B}} - [(\chi^2_{\text{min}})_{\text{A}} + (\chi^2_{\text{min}})_{\text{B}}]$. It has a χ^2 distribution with number of degrees of freedom NDF $= P_{\text{A}} + P_{\text{B}} - P_{\text{A+B}}$, where P_{A}, P_{B} and $P_{\text{A+B}}$ are, respectively, the number of parameters in the fits of A, B and A + B data [32].

[7]In our figures we considered Δm^2 in the range 10^{-2}–10^2 eV^2. For simplicity, we neglected the small Δm^2 dependence of the CHOOZ exclusion curve for $\Delta m^2 \lesssim 4 \times 10^{-2}$ eV^2 (see Fig. 55 of Ref. [26]).

the case of no oscillations do not allow us to exclude this possibility.

From the comparison of Eq. (12) and Fig. 2, one can see that the results of the Chooz and the Gallium radioactive source experiments are compatible only at the 2σ level. In fact the parameter goodness-of-fit reported in Table III shows a tension between Gallium and Chooz data under the hypothesis of neutrino oscillations.

Figure 8 shows the allowed regions in the $\sin^2 2\vartheta - \Delta m^2$ plane obtained with the combined least-squares fit of Gallium and Chooz data. The values of $\chi^2_{\rm min}$ and goodness of fit and the best-fit values of the mixing parameters are given in Table III. It is clear that the combined fit is not good, since the results of Chooz and the Gallium radioactive source experiments are in contradiction regarding neutrino disappearance. The marginal allowed ranges of $\sin^2 2\vartheta$ and Δm^2 in Table V are of little interest, since the minima of the corresponding $\Delta\chi^2$'s in Fig. 8 are very shallow, except for the upper bound on $\sin^2 2\vartheta$ driven by Chooz data. As one can see from the allowed regions in the $\sin^2 2\vartheta - \Delta m^2$ plane in Fig. 8, the Chooz bound on $\sin^2 2\vartheta$ in Eq. (12) is weakened by the results of the Gallium radioactive source experiments in a significant way only for $\Delta m^2 \gtrsim 10^{-1}$ eV^2 at the 1σ level.

Finally, we performed a combined fit of the results of Bugey, Chooz, and Gallium data. The resulting allowed regions in the $\sin^2 2\vartheta - \Delta m^2$ plane are shown in Fig. 9. The best-fit values and the marginal allowed ranges of the mixing parameters are listed, respectively, in Tables III and V. One can see that the Gallium and Chooz data tend to compensate each other, leading to results which are similar to those obtained in the analysis of Bugey data alone. The value of the parameter goodness-of-fit reported in Table III does not allow us to exclude the compatibility of the Bugey, Chooz and Gallium data under the hypothesis of neutrino oscillations. Also the goodness-of-fit obtained in the case of no oscillations, given in Table III, is acceptable. Therefore, we can only conclude that the combined analysis of all the experimental data that we have considered is compatible both with the case of no oscillations and with the hint in favor of neutrino oscillations with $0.02 \lesssim \sin^2 2\vartheta \lesssim 0.08$ and $\Delta m^2 \approx 1.8$ eV^2 found in the analysis of Bugey data.

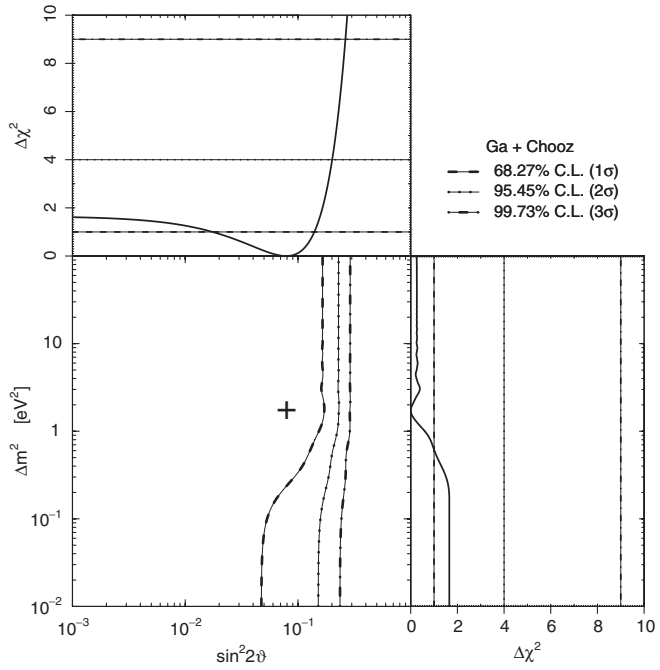

FIG. 8. Allowed regions in the $\sin^2 2\vartheta - \Delta m^2$ plane and marginal $\Delta\chi^2$'s for $\sin^2 2\vartheta$ and Δm^2 obtained from the combined fit of the results of the two GALLEX ^{51}Cr radioactive source experiments, the SAGE ^{51}Cr and ^{37}Ar radioactive source experiments and the Chooz reactor experiment. The best-fit point corresponding to $\chi^2_{\rm min}$ is indicated by a cross.

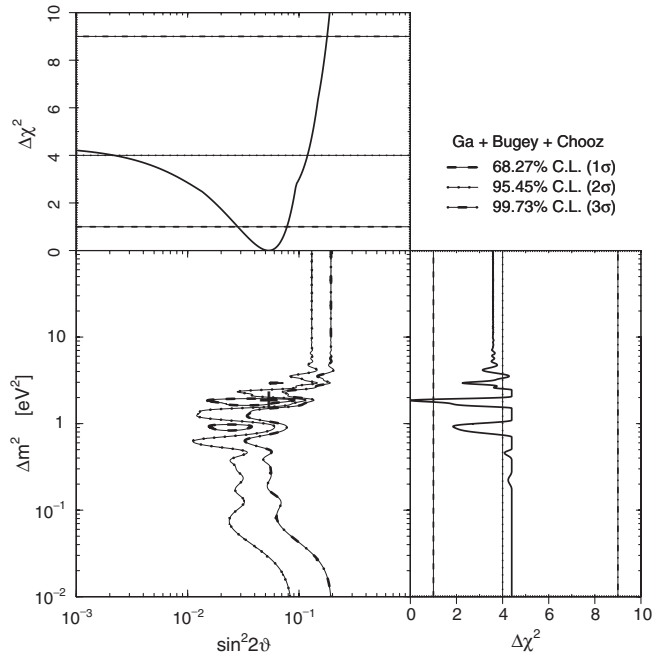

FIG. 9. Allowed regions in the $\sin^2 2\vartheta - \Delta m^2$ plane and marginal $\Delta\chi^2$'s for $\sin^2 2\vartheta$ and Δm^2 obtained from the combined fit of the results of the two GALLEX ^{51}Cr radioactive source experiments, the SAGE ^{51}Cr and ^{37}Ar radioactive source experiments and the Bugey and Chooz reactor experiments. The best-fit point corresponding to $\chi^2_{\rm min}$ is indicated by a cross.

V. CONCLUSIONS

We interpreted the deficit observed in the Gallium radioactive source experiments as a possible indication of the disappearance of electron neutrinos. We have analyzed the data in the effective framework of two-neutrino mixing, which describes neutrino oscillations due to a Δm^2 that is much larger than the solar and atmospheric ones. We found that there is an indication of electron neutrino disappearance due to neutrino oscillations with $\sin^2 2\vartheta \gtrsim 0.03$ and $\Delta m^2 \gtrsim 0.1$ eV^2. We have also studied the compatibility of the data of the Gallium radioactive source experiments

with the data of the Bugey and Chooz reactor short-baseline antineutrino disappearance experiments in the same effective framework of two-neutrino mixing, in which the disappearance of neutrinos and antineutrinos are equal. We found that the Bugey data present a hint of neutrino oscillations with $0.02 \lesssim \sin^2 2\vartheta \lesssim 0.08$ and $\Delta m^2 \approx 1.8\ \mathrm{eV}^2$, which is compatible with the region of the mixing parameters allowed by the analysis of the data of the Gallium radioactive source experiments. We have also performed combined analyses of the Bugey and Chooz data, of the Gallium and Bugey data, of the Gallium and Chooz data, which show that the Bugey and Chooz data are compatible, the Gallium and Bugey data are compatible, and the Gallium and Chooz data are marginally compatible. The weak indication in favor of neutrino oscillations found in the analysis of the Bugey data persists in the combined analyses of the Bugey data with the Gallium and Chooz data. However, we cannot exclude the absence of oscillations.

From a physical point of view, a hint in favor of short-baseline neutrino oscillations generated by $\Delta m^2 \gtrsim 0.1\ \mathrm{eV}^2$ is extremely interesting. This squared-mass difference is too large to be compatible with the three-neutrino mixing scheme inferred from the observation of neutrino oscillations in solar, very-long-baseline reactor, atmospheric and long-baseline accelerator experiments, in which there are only two independent squared-mass differences, $\Delta m^2_{\mathrm{SOL}} \approx 8 \times 10^{-5}\ \mathrm{eV}^2$ and $\Delta m^2_{\mathrm{ATM}} \approx 3 \times 10^{-3}\ \mathrm{eV}^2$. Therefore, the results of our analysis indicate the possible existence of at least one light sterile neutrino ν_s (see Refs. [5,6,11]). We think that it is very important to explore this intriguing hint of new physics beyond the standard model.

As already discussed in Ref. [24], short-baseline $\overset{(-)}{\nu}_e \to \overset{(-)}{\nu}_s$ transitions have an influence on the interpretation of all experiments with an initial $\overset{(-)}{\nu}_e$ beam. In the existing solar and atmospheric neutrino experiments the survival probability of $\overset{(-)}{\nu}_e$ is the averaged one in Eq. (11). However, the uncertainties of the experimental data and our knowledge of the initial flux do not allow us to exclude $\overset{(-)}{\nu}_e \to \overset{(-)}{\nu}_s$ transitions at the level of about 20% in the case of solar neutrinos [38] and about 30% (see Ref. [11]) in the case of atmospheric neutrinos.

Future experiments which are well suited for finding small $\overset{(-)}{\nu}_e \to \overset{(-)}{\nu}_s$ transitions are those with a source producing a $\overset{(-)}{\nu}_e$ flux which is known with high accuracy. Since sterile neutrinos are invisible, $\overset{(-)}{\nu}_e \to \overset{(-)}{\nu}_s$ transitions can be revealed either by measuring a disappearance of $\overset{(-)}{\nu}_e$'s without $\overset{(-)}{\mu}$ or $\overset{(-)}{\tau}$ production in the detection process or by measuring a disappearance of $\overset{(-)}{\nu}_e$'s due to oscillations with a squared-mass difference much larger than $\Delta m^2_{\mathrm{SOL}}$ and $\Delta m^2_{\mathrm{ATM}}$. We are aware of the following possibilities: beta-beam experiments [39] which have a pure ν_e or $\bar{\nu}_e$ beam from nuclear decay (see the reviews in Refs. [40,41]); neutrino factory experiments in which the beam is composed of ν_e and $\bar{\nu}_\mu$, from μ^+ decay, or $\bar{\nu}_e$ and ν_μ, from μ^- decay (see the review in Ref. [40,42]); Mossbauer neutrino experiments, with a $\bar{\nu}_e$ beam produced in recoilless nuclear decay and detected in recoilless nuclear antineutrino capture [43]; the LENS detector [44,45] with an artificial Megacurie ν_e source [46]. Let us also notice the very interesting possibility to reveal the existence of sterile neutrinos in the flux of high-energy astrophysical neutrinos after their passage through the Earth by measuring the peculiar matter effects [47,48].

ACKNOWLEDGMENTS

We would like to express our gratitude to Y. Declais for giving us detailed information on the Bugey experiment. M. A. Acero would like to thank the International Doctorate on AstroParticle Physics (IDAPP) for financial support. C. Giunti would like to thank the Department of Theoretical Physics of the University of Torino for hospitality and support.

[1] S. Abe *et al.* (KamLAND), Phys. Rev. Lett. **100**, 221803 (2008).
[2] P. Adamson *et al.* (MINOS), Phys. Rev. D **77**, 072002 (2008).
[3] S. M. Bilenky and B. Pontecorvo, Phys. Rep. **41**, 225 (1978).
[4] S. M. Bilenky and S. T. Petcov, Rev. Mod. Phys. **59**, 671 (1987).
[5] S. M. Bilenky, C. Giunti, and W. Grimus, Prog. Part. Nucl. Phys. **43**, 1 (1999).
[6] M. Gonzalez-Garcia and Y. Nir, Rev. Mod. Phys. **75**, 345 (2003).
[7] C. Giunti and M. Laveder, in *Developments in Quantum Physics–2004*, edited by F. Columbus and V. Krasnoholovets (Nova Science Publishers, Inc., Hauppauge, New York, 2003), pp. 197–254
[8] M. Maltoni *et al.*, New J. Phys. **6**, 122 (2004).
[9] G. L. Fogli *et al.*, Prog. Part. Nucl. Phys. **57**, 742 (2006).
[10] A. Strumia and F. Vissani, arXiv:hep-ph/0606054.
[11] C. Giunti and C. W. Kim, *Fundamentals of Neutrino*

Physics and Astrophysics (Oxford University Press, New York, 2007).
[12] A. Aguilar *et al.* (LSND), Phys. Rev. D **64**, 112007 (2001).
[13] J. N. Abdurashitov *et al.*, Phys. Rev. C **73**, 045805 (2006).
[14] A. Aguilar-Arevalo *et al.* (MiniBooNE), Phys. Rev. Lett. **98**, 231801 (2007).
[15] P. Anselmann *et al.* (GALLEX), Phys. Lett. B **342**, 440 (1995).
[16] W. Hampel *et al.* (GALLEX), Phys. Lett. B **420**, 114 (1998).
[17] J. N. Abdurashitov *et al.* (SAGE), Phys. Rev. Lett. **77**, 4708 (1996).
[18] J. N. Abdurashitov *et al.* (SAGE), Phys. Rev. C **59**, 2246 (1999).
[19] W. Hampel *et al.* (GALLEX), Phys. Lett. B **447**, 127 (1999).
[20] J. N. Abdurashitov *et al.*, Astropart. Phys. **25**, 349 (2006).
[21] G. Fogli *et al.*, arXiv:hep-ph/0605186.
[22] M. Laveder, Nucl. Phys. B, Proc. Suppl. **168**, 344 (2007).
[23] C. Giunti and M. Laveder, Mod. Phys. Lett. A **22**, 2499 (2007).
[24] C. Giunti and M. Laveder, Phys. Rev. D **77**, 093002 (2008).
[25] B. Achkar *et al.* (Bugey), Nucl. Phys. **B434**, 503 (1995).
[26] M. Apollonio *et al.* (CHOOZ), Eur. Phys. J. C **27**, 331 (2003).
[27] J. N. Bahcall, Phys. Rev. C **56**, 3391 (1997).
[28] V. A. Kuzmin, Sov. Phys. JETP **22**, 1051 (1966) [Zh. Eksp. Teor. Fiz. **49**, 1532 (1965)].
[29] F. Kaether, Ph.D. Thesis (in German), 2007; URL: http://www.ub.uni-heidelberg.de/archiv/7501/.
[30] R. L. Hahn, *Neutrino 2008, 2008* (Christchurch, New Zealand, 2008); URL: http://www2.phys.canterbury.ac.nz/~jaa53/presentations/Hahn.pdf .
[31] W. M. Yao *et al.*, J. Phys. G **33**, 1 (2006); URL: http://pdg.lbl.gov.
[32] M. Maltoni and T. Schwetz, Phys. Rev. D **68**, 033020 (2003).
[33] J. N. Bahcall, P. I. Krastev, and E. Lisi, Phys. Lett. B **348**, 121 (1995).
[34] C. Bemporad, G. Gratta, and P. Vogel, Rev. Mod. Phys. **74**, 297 (2002).
[35] W. Grimus and T. Schwetz, Eur. Phys. J. C **20**, 1 (2001).
[36] Y. Declais (private communication).
[37] G. J. Feldman and R. D. Cousins, Phys. Rev. D **57**, 3873 (1998).
[38] J. N. Bahcall, M. C. Gonzalez-Garcia, and C. Pena-Garay, J. High Energy Phys. 08 (2004) 016.
[39] P. Zucchelli, Phys. Lett. B **532**, 166 (2002).
[40] C. Albright *et al.* (Neutrino Factory/Muon Collider), arXiv:physics/0411123.
[41] C. Volpe, J. Phys. G **34**, R1 (2007).
[42] M. Apollonio *et al.*, arXiv:hep-ph/0210192.
[43] R. S. Raghavan, arXiv:hep-ph/0601079.
[44] R. S. Raghavan, Phys. Rev. Lett. **78**, 3618 (1997).
[45] R. S. Raghavan *et al.* (2002), URL: http://lens.in2p3.fr/lens-rep-02.pdf.
[46] C. Grieb, J. Link, and R. S. Raghavan, Phys. Rev. D **75**, 093006 (2007).
[47] H. Nunokawa, O. L. G. Peres, and R. Z. Funchal, Phys. Lett. B **562**, 279 (2003).
[48] S. Choubey, J. High Energy Phys. 12 (2007) 014.